Nanostructured Inorganically Pillared Layered Metal(IV) Phosphates

Pascual Olivera-Pastor, Pedro Maireles-Torres, Enrique Rodríguez-Castellón, and Antonio Jiménez-López*

Departamento de Quimica Inorganica, Cristalografia y Mineralogia, Universidad de Malaga, 29071 Malaga, Spain

Thierry Cassagneau, Deborah J. Jones, and Jacques Rozière*

Laboratoire des Agrégats Moléculaires et Matériaux Inorganiques, URA CNRS 79, Université Montpellier 2, Place E. Bataillon, 34095 Montpellier Cedex 5, France

Received February 23, 1996. Revised Manuscript Received April 29, 1996[⊗]

This article reviews the synthesis, characterization and ion-exchange, ion-transport, sorptive, and catalytic properties of inorganically pillared layered metal(IV) phosphates, typified by $Zr(HPO_4)_2 \cdot H_2O$. Porous nanostructures are generally prepared from metal(IV) phosphates either by ion exchange of polynuclear species or by intercalation from solutions of condensed species obtained by the hydrolysis of organometallic precursors using sol−gel methods, followed by thermal treatment to eliminate organic moieties, condense hydroxyl groups, eliminate water, and consolidate the structure by grafting the pillar to the layer. The different strategies devised to overcome the problem presented by the high layer charge density of α- and γ-structured phosphates in obtaining porous solids, including exfoliation and local surface growth of pillaring ions, and modification of the zirconium phosphate matrix to reduce the cation-exchange capacity, are described. Structural and textural characteristics of Al, Cr, mixed Al−Cr, Fe−Cr, Ga−Al and of Si-pillared phosphates obtained from XAFS, XPS, and MAS NMR are presented, and the perspectives of nanocomposite pillared layered solids in general are discussed in the current context of mesoporous solids synthesized using templating routes.

Introduction

Parallel to the development of new methods for zeolite synthesis, other routes have been explored appropriate for the synthesis of porous materials for use as catalysts in the petrochemical and chemical industries and separation technologies in particular. One of the most important concerns the preparation of pillared layered structures (PLS) derived from layered materials, mainly clays,[1−5] but also including other hosts, such as niobates,[6] silicic acids,[7] phosphates, and layered double hydroxides.[8] A further alternative represented by the MCM41S family of mesoporous silicas[9] has led to an enormous surge of interest in templating routes to mesoporous solids in general.[10]

Pillared layered solids are formed by intercalation of large polymeric inorganic cations in the interlayer region of layered solids. After calcination, the precursor cations are transformed to the respective metal oxide nanoclusters, which prop the layers permanently apart. The presence of inorganic species acting as pillars and interacting strongly with the layers gives rise to thermally stable materials of high surface area and pore volume accessible for ion exchange, adsorption, and catalysis. A broad spectrum of pillaring ions (Zr, Cr, Al, Si, Fe, Ga, etc.)[11] and a range of layered hosts provides the opportunity in pillared layered chemistry for creating numerous chemical combinations, the full potential of which in designing active porous solids is only now being fully realized. In Europe, university and industrial groups have been working together over the past 4 years within the framework of a European Union funded Concerted Action on Pillared Layered Structures[12] (CEA-PLS) to explore new pillaring methods, new host structures, new pillaring species, and new techniques for the characterization of PLS and to investigate the activity of PLS in catalysis and separation processes, their electrochemical activity, and their use as template solids. Within the CEA-PLS, groups at the Universities of Málaga and Montpellier and at the CNR in Rome have developed the pillaring of layered phosphates with inorganic species from the pioneering work of Clearfield.[13] The use of phosphonates to produce organically pillared phosphates has been largely developed in Europe by Alberti[14,15] and in the US by Clearfield[16,17] and others[18] and is not further treated here in detail.

Metal(IV) layered phosphates are unable to swell in water, unlike smectite clays, and it is therefore necessary to preswell them with alkylamines, alcohols, or amino acids before intercalating large cations.[19] The α structure of zirconium phosphate (α-ZrP) delaminates in water by addition of *n*-propylamine at 50% of the saturation capacity to form stable colloidal suspensions,[20] which assists the intercalation of many large cations capable of acting as pillaring agents.

Of the layered metal(IV) phosphates, α-ZrP has been the most extensively studied, partly because its structure has been fully determined.[21,22] Layered metal (IV) phosphates are good ion exchangers[23] and host matrixes

[⊗] Abstract published in *Advance ACS Abstracts,* July 15, 1996.

S0897-4756(96)00156-1 CCC: $12.00

for the preparation of nanocomposite solids via the intercalation of organic[24] or inorganic species.[17b] In recent years, the modification of the interlayer region of α-ZrP to give solids composed of alternating inorganic and organic layers by intercalation/in situ formation of organic polymers has also received significant attention.[25] Zirconium phosphate is also active as a catalyst.[26−29]

A variety of different methods of pillaring have been conceived according to the polymeric intercalant species used. The preparation strategies for pillaring phosphates are discussed in this review. Characterization of PLS is a major challenge requiring the use of a number of complementary techniques. We describe here approaches to the structural characterization of some of the pillaring species present in the interlayer region by using techniques such as X-ray photoelectron spectroscopy (XPS), MAS-NMR, and X-ray absorption spectroscopy (XAS), which supply information about the chemical environment of metallic cations and, sometimes, on their interaction with the layer of the host matrix. Some of the properties of the resulting pillared materials, including their acid−base character, ion exchange characteristics, and use as template solids are presented in a final section.

Preparation and Characterization of Pillared Metal(IV) Phosphates

Pillared Phosphates from Inorganic Pillar Precursors. *Aluminum Oxide Pillared Metal(IV) Phosphates.* Much attention has been paid to the preparation of pillared compounds using the Keggin-like ion $[AlO_4Al_{12}(OH)_{24}(H_2O)_{12}]^{7+}$, "$Al_{13}$". It is one of the best characterized oligomeric cationic species, both in the solid state[30] and in solution.[31] Clearfield and Roberts[13] first reported the pillaring of layered zirconium and titanium phosphates (ZrP, TiP) with Al_{13}, which was intercalated by contacting, at 70 °C, the *n*-butylamine intercalates with a solution of basic aluminum chloride hydroxide (from Reheis), known as chlorhydrol and empirically formulated as $Al_2(OH)_5Cl$. Most intercalated α-ZrP samples had interlayer distances (calculated from the first observed 00l diffraction line) ranging between 13 and 16 Å; these were the expected values considering that the Al_{13} ion can be described as a prolate spheroid of dimensions ∼9.5 × 7 Å and that the phosphate layer thickness is close to 6.3 Å. However, in some cases, highly crystalline α-ZrP formed intercalation compounds with interlayer distances of 24−30 Å, although after calcination at 400 °C all the α-ZrP phases had low surface area (30−35 $m^2\ g^{-1}$) and no capacity to intercalate small polar molecules. These first alumina-cross-linked phosphates were therefore nonporous solids, in which the available interlayer space was completely filled by the aluminum oxide pillars ("stuffed" structures). Conversely, the analogous α- and γ-pillared titanium compounds showed high BET surface areas (up to 183 $m^2\ g^{-1}$) as compared to the original phosphate (∼10 $m^2\ g^{-1}$) and sorbed relatively large molecules. The pore size distribution of pillared TiP is characteristic of a mesoporous structure with a range of pore radii between 10 and 100 Å and an appreciable fraction of micropores.

Pillaring of α-SnP with Al_{13} was studied at room temperature using aged solutions of $AlCl_3{\cdot}6H_2O$ partially neutralized with NaOH (Al_{13} solutions) or solutions of chlorhydrol (Chlor).[32,33] The phosphate was first colloidized with *n*-propylamine and then *n*-propylammonium ions exchanged by tetramethylammonium ions before contacting the phosphate with the oligomer solution, in order to improve ordering in the pillared materials. Greater retention of aluminum oligomer occurred from chlorhydrol solutions. At the plateau of the uptake curves, samples displayed interlayer distances of 17.7 Å for Al_{13}−SnP precursors and 24.2 Å for Chlor−SnP precursors, compatible with a monolayer of Al_{13} oligomers intercalated in Al_{13}−SnP and a bilayer in Chlor−SnP, although, as revealed by ^{27}Al NMR studies of chlorhydrol solutions,[34] other aluminum species might be also present in the latter. Nevertheless, calcination of these two precursors at 400 °C leads to materials with similar interlayer distances (about 12 Å, Figure 1), which suggests that similar pillaring species are formed. The interaction of alumina pillars with the phosphate layer is so strong that no segregation of Al_2O_3 was observed beyond 400 °C, SnO_2 and aluminum phosphate being identified by X-ray diffraction (XRD) after calcination at 1000 °C.

Alumina pillared α-SnP materials (precursors calcined at 400 °C) have a BET surface area of 190−230 $m^2\ g^{-1}$ and are mesoporous with a small fraction of micropores (0.02 $cm^3\ g^{-1}$). Most of the pores (>50%) had radii in the range 15−40 Å (Figure 2). Their mesoporosity may originate from end-side particle

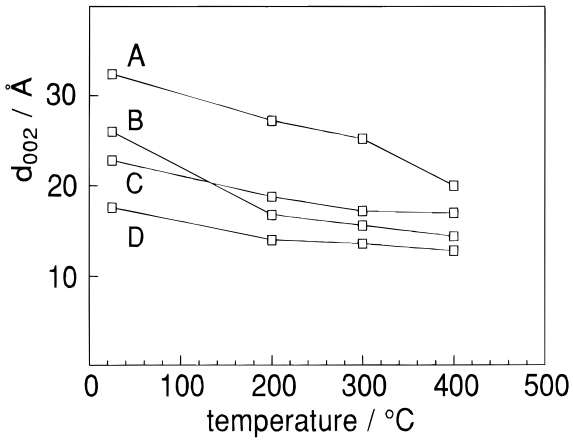

Figure 1. Evolution of the basal spacing with temperature for aluminum oligomer intercalates: (A) α-SnP with buffered acetate solution; (B) α-SnP with chlorhydrol solution; (C) α-ZrP with fluorinated Al_{24} solution; (D) α-SnP with partially hydrolyzed solution.

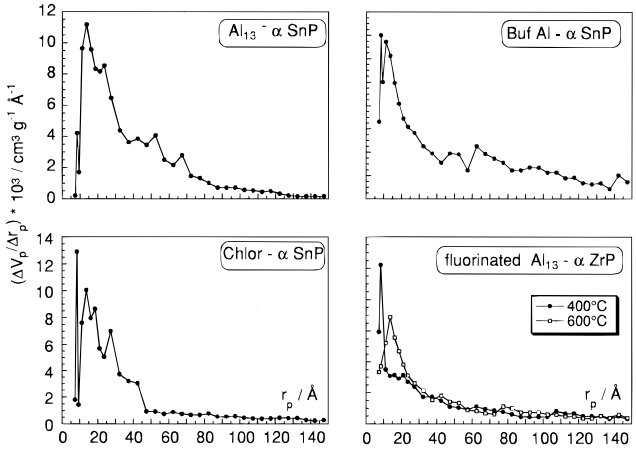

Figure 2. Pore size distributions of alumina pillared phosphates (samples as in Figure 1; r_p = pore radius).

interactions, a part of which could be internal pores formed by cut layers owing to hydrolysis.

From calculations based on the dimensions of the Al_{13} ion and the distance between fixed charges on the phosphate surface (5.3 Å for α-ZrP), it has been suggested[15,16] that this oligomer is too large to generate interlayer porosity in a layered phosphate so resistant to hydrolysis as α-ZrP and that the existence of porosity in pillared tin and titanium phosphates is ultimately due to the loss of phosphate because of their more hydrolyzable nature. Indeed, the stability to hydrolysis decreases in the order[15]

$$ZrP \gg TiP > SnP > PbP \gg GeP$$

However, it should also be taken into account that pillared phosphates lose about 30% of the sample weight as water upon calcination at 400 °C and, hence, a considerable decrease in the lateral dimension of the pillar would be expected in the process of its transformation to aluminum oxide. On the other hand, antimony phosphate, $HSb(PO_4)_2$, which has the same layer structure as ZrP but with only half the exchangeable hydrogen ions, also gives rise to stuffed products after insertion of Al_{13} and thermal treatment.[16] Clearly, other factors, in addition to the loss of phosphate, affect the porous nature of pillared phosphates.

One way to improve the interlayer porosity consists of intercalating more extended oligomers than Al_{13}, such as Al_{24}, thought to form by condensation of two Al_{13} ions,[35] in order to reduce the strong interlayer contraction observed upon calcination. Performing the intercalation reaction under reflux and buffering with acetate leads to more homogeneous α-SnP derivatives with higher Al contents and *d* spacings reaching 30.3 Å. The resulting pillared materials showed greater free heights,[36] enhanced microporosity (>20%), and very narrow pore size distributions, most of the pores being centered between $r_p = 8.5-11.3$ Å (Figure 2).

^{27}Al MAS NMR provided the first evidence that at least part of the aluminum is intercalated as Al_{13} ion in α-ZrP by showing resonances characteristic of tetrahedral and octahedral sites.[37] MAS-NMR studies of alumina pillared α-SnP and α-ZrP have provided information about the nature of the interaction of aluminum species with the host (Figure 3). This interaction produced a shift of the ^{31}P signal toward higher field positions. In addition to the resonance lines typical of octahedral and tetrahedral aluminum, the ^{27}Al spectra displayed a third resonance at 30−40 ppm that increases in intensity after calcination at 400 °C, and it was concluded that aluminum oxide pillars are cross-linked to the phosphate layer through pentacoordinated Al. The fact that larger displacements of the chemical shift were observed for α-ZrP derivatives than for those of α-SnP indicates that the interaction of aluminum with the phosphate layer is stronger in α-ZrP. This strong interaction could be responsible for the formation of stuffed structures in α-ZrP.

These considerations led us to suppose that the porosity of aluminum oxide pillared layered phosphates is not only related to the hydrolytic stability of the phosphate but also to the strength of the Al−O−P linkages formed between the interlayer aluminum oxide and the layered matrix. Recently, it has been demonstrated that the incorporation of F^- ions into the framework of the aluminum oligomers by partially substituting OH^- groups considerably reduces the interaction of the aluminum oxide pillar with the layers of α-ZrP and avoids rapid spreading of the aluminum oxide throughout the interlayer upon calcination, since the formation of Al−O−P linkages is substantially decreased.

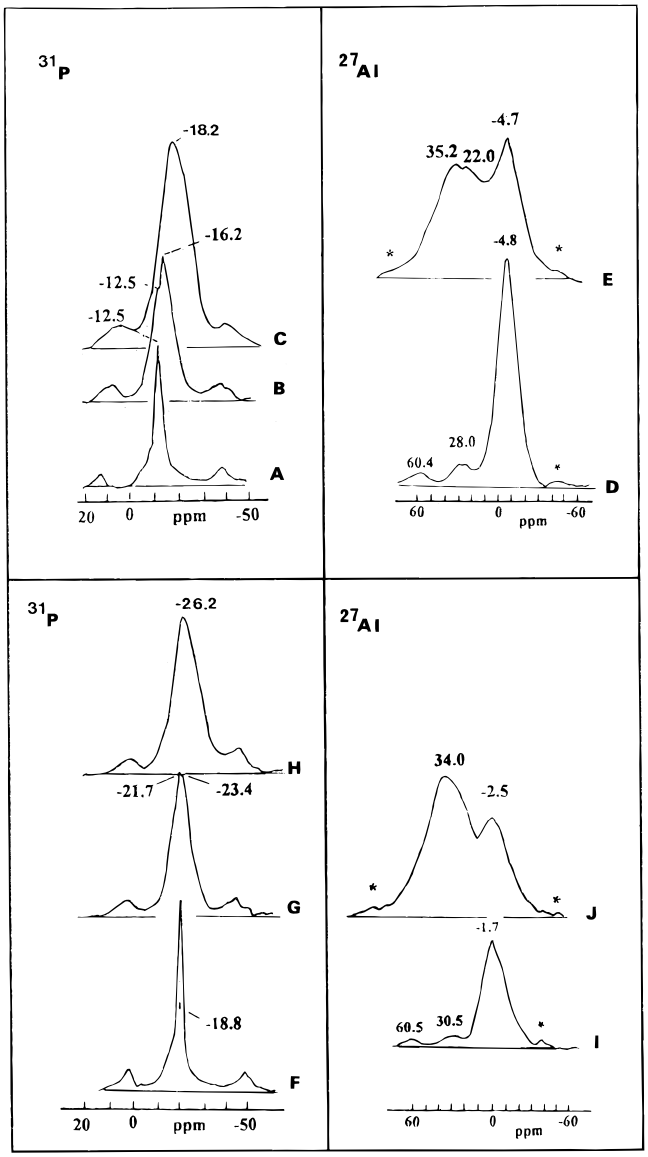

Figure 3. ^{31}P and ^{27}Al MAS-NMR spectra of (A) α-SnP; (B) Al_{13}−SnP; (C) sample B at 400 °C; (D) Al_{13}−SnP, (E) sample D at 400 °C; (F) α-ZrP; (G) CHL−ZrP; (H) sample G at 400 °C; (I) CHL−ZrP; (J) sample I at 400 °C.

By contacting colloidal α-ZrP with a solution of Al_{24} and following consecutive reflux-hydrothermal treatments in the presence of F^-, a single-phase material with basal spacing of 21.3 Å (Figure 1) was obtained.[38] Both the thermal stability and porous structure were undoubtedly improved by this procedure as compared to pillared compounds prepared by conventional methods. At 400 °C, the fluorinated alumina pillared α-ZrP had an interlayer distance of 17.3 Å (Figure 1), which corresponds to a free height of ∼11 Å, a micropore volume close to 0.1 $cm^3\ g^{-1}$ and a very narrow pore size distribution, centered at *ca.* 8 Å radius (Figure 2). The microporosity displayed by this product is of the same order as that reported for pillared clays.[2]

It has been shown by XPS studies that the layer structure is preserved after pillaring with aluminum

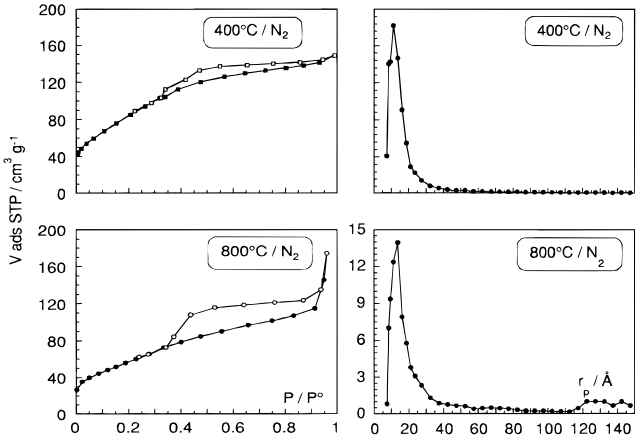

Figure 4. N_2 adsorption/desorption isotherms and pore size distributions of a chromia pillared α-ZrP material calcined at two different temperatures (r_p = pore radius).

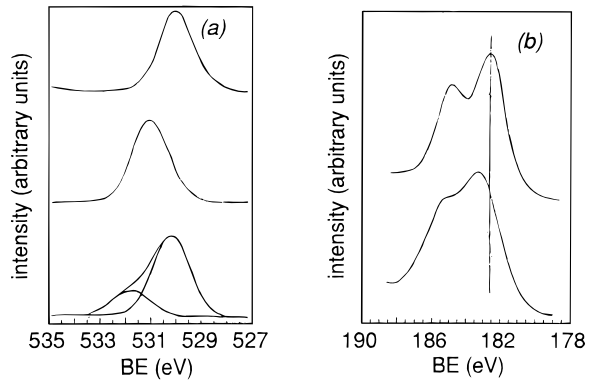

Figure 5. (a) O1s XPS spectra: upper, Cr_2O_3; middle, Cr-pillared SnP; lower, α-SnP and (b) Zr3d XPS spectra: upper, α-ZrP; lower, Cr-pillared ZrP.

oxides, since the binding energies of P2p and Zr3d are coincident with those found for the pristine phosphates.[39] This technique also allowed the formation of side products, such as aluminum phosphate, to be ruled out, at least up to 1000 °C. Measurements of the modified Auger parameter for Al [40] showed values in the range 1460.8−1461.1 eV, which are intermediate between those of octahedral and tetrahedral aluminum of well-characterized aluminosilicates, as a consequence of the strong interaction established between aluminum oxide and the phosphate layer.

Chromium Oxide Pillared Metal(IV) Phosphates. The use of chromium acetate as a method for insertion of Cr^{3+} species into a layered phosphate was first demonstrated by Bibby,[41] and it has now been developed into a general method [42−43] of preparation of chromia pillared materials by in situ polymerization of $Cr(OAc)_3$ on a delaminated host surface. Contacting chromium acetate solutions with α-$ZrNaH(PO_4)_2{\cdot}5H_2O$[41] or hexylamine-α-ZrP[16] intercalates gave rise to amorphous or low *d* spacing pillared materials with BET surface area <130 $m^2\ g^{-1}$. This may be due to the restricted interlayer space of these moderately expanded exchangers which impedes ordered hydrolysis of chromium acetate and favors the formation of different interlayer fragments. However, when chromium acetate was refluxed with colloidal suspensions of *n*-propylamine intercalated α-SnP or α-ZrP, ordered solids with a single type of intercalated chromium oligomer were obtained. When using this method to pillar antimony phosphate, $HSb(PO_4)_2$, Clearfield et al.[16] obtained two types of

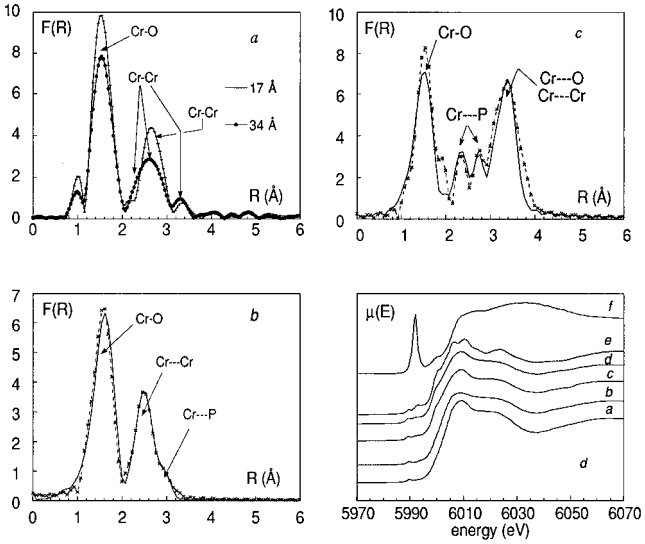

Figure 6. (a) Fourier transformed XAFS spectra of chromia pillared precursor phases with interlayer distances 17 and 34 Å. (b) Comparison of the experimental (×) and calculated (—) Fourier transformed spectra of chromia pillared ZrP calcined at 400 and (c) 800 °C. (d) Near-edge region of (a, b)17 and 34 Å precursor phases, (c, d) chromia pillared ZrP calcined at 400 and 800 °C, (e) Cr_2O_3, and (f) $K_2Cr_2O_7$.

chromia pillared materials depending on the chromium-to-phosphate ratio in the initial reagent mixture, the highest porosity material having a BET surface area of 132 $m^2\ g^{-1}$ and a pore volume of 0.099 $cm^3\ g^{-1}$, of which about 48% could be attributed to micropores. The uptake curves of chromium in α-SnP[44] and α-ZrP[45] hosts are typical of species association occurring during the exchange reaction as described by Giles et al.[46] Depending on Cr/P ratios and Cr concentrations, a series of polyhydroxy acetate−Cr^{3+} intercalated precursor materials was obtained, with interlayer distances ranging from 13.0 to 39.0 Å. Calcination under N_2 at 400 °C led to a chromia pillared materials with free heights of 3.5−20.5 Å. These nanoscale oxide-pillared compounds were predominantly mesoporous solids with micropore contributions of 0.05−0.12 $cm^3\ g^{-1}$ and BET surface areas of 200−390 $m^2\ g^{-1}$. The pore size distributions, calculated using a cylindrical pore model,[47] were very narrow, and this observation together with the above free heights is evidence in favor of some of the pores in the internal surface being true mesopores. Calcination of α-ZrP derivatives at 800 °C led to amorphous materials, but with virtually the same narrow pore size distributions and surface areas >200 $m^2\ g^{-1}$ (Figure 4). This poses the problem of whether XRD alone is a useful technique for the assessment of porosity induced by a pillaring mechanism. The amorphous nature of the porous chromia pillared phosphate may be rationalized by assuming that it arises from end-to-end sintered particles which are so small (<50 Å) as to give only ill-defined ("amorphous") XRD patterns but yet do not preclude long-range order. Alternatively, shrinkage of the pillars at this high temperature may rotate adjacent layers in opposite directions or otherwise cause misalignment so destroying Bragg reflections.

X-ray photoelectron spectroscopy has been used to examine the oxidation state and chemical environment of the elements present on the surface of chromia-pillared metal(IV) phosphates.[39] The results confirm that all the materials contain Cr(III) ions only in an oxidic environment. Cr2p binding energies and the

Auger parameter for oxygen shows the insertion of chromium species into the phosphate network to form single-phase materials, as previously inferred from XRD studies; no separate Cr_2O_3 domains were present (Figure 5).

An X-ray absorption spectroscopic study provided detailed information on the nature of the chromium oligomers in the intercalated precursors and on the environment of chromium in calcined phases.[48] The Fourier transformed EXAFS spectra of two intercalated phosphate materials with basal spacings of 17 and 34 Å, respectively, are shown in Figure 6a. For the less expanded α-ZrP prepared at lower Cr/Zr ratios, the EXAFS result is in agreement with the intercalation of the cyclic trimer **1**, whereas the use of a higher Cr/Zr

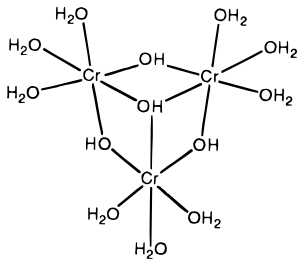

1

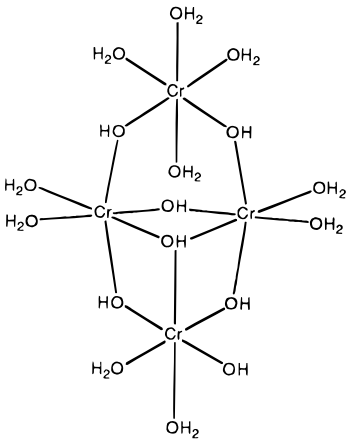

2

ratio in the synthesis leads to an intercalate with an interlayer distance of 34 Å, and for which EXAFS data (coordination numbers, bond lengths) are consistent with the presence of the open tetramer **2**. After calcination, the environment of chromium, Figure 6b, is very similar to that of α-Cr_2O_3 with, in addition, a phosphorus atom shell at a distance (3.25 Å) compatible with coordination of the pillar to the phosphate layer via Cr−O−P bonds. This covalent bonding or cross-linking can explain the high thermal stability of chromia-pillared zirconium phosphate. After amorphization at 800 °C, the pillar species can be described as an oxide−phosphate nanoparticle with contributions to the EXAFS from bidentate PO_4^{3-} groups, Figure 6c. Neither the near-edge (Figure 6d) nor EXAFS regions provides any evidence for the presence of Cr^{VI}, unlike the conclusions of a previous XAS study on the insertion of hydroxyoxychromium(III) cations into a bentonite that the chromia pillars formed after calcination at 250 °C consisted of mixed valence $Cr^{III}Cr^{VI}$ species.[49] Here, oxidation of Cr(III) is more probably due to the presence

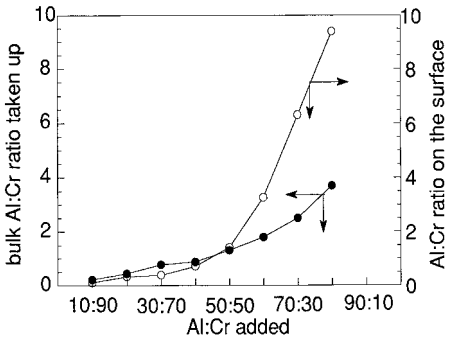

Figure 7. Bulk (●) and surface (○) Al/Cr ratios versus Al/Cr added in mixed Al/Cr pillared α-ZrP.

of traces of manganese oxides in the bentonite host,[50] rather than being a consequence of the pillaring procedure.

Mixed-Metal Oxide Pillared Metal(IV) Phosphates. The possibility of incorporating a large number of metal cations in the pillaring oxide particle provide the opportunity of creating multifunctional catalysts. Few metal cations form positively charged polymeric species in solution before precipitation, but the use of such mixed oligomer solutions has already permitted the insertion of a wide variety of mixed oxides, mainly into clays.[51−54]

Since Cr^{3+} can form solid solutions with many other cations and since chromium(III) acetate solutions are appropriate media for the in situ growth of oligomeric species on the surface phosphate at controlled pH, three different mixed M(III)/Cr(III) solutions: Al/Cr,[55] Fe/Cr,[56] and Ga/Cr[57] were assayed as pillaring solutions. The intercalation reactions of mixed oligomers were carried out, at reflux temperature, using solutions buffered with acetate at pH = 4−4.5. In addition to regulating the pH, acetate forms part of the framework of the mixed oligomers by acting as a bidentate ligand linked predominantly to chromium, and is easily eliminated by thermal treatment to leave interlayer voids. Using XPS, it was possible to determine the range of composition in which mixed oligomers are intercalated (Figure 7). For high M(III)/Cr(III) ratios (>70/30), the bulk composition diverged from the surface composition as a consequence of the different affinity shown by the phosphate surface toward metal ions. Materials with M(III)/Cr(III) ratios >60/40 usually presented low surface area and porosity, and this was interpreted as due to the accumulation of one of the metal ions on the phosphate surface which impeded the access of the nitrogen molecules to the internal pores. Conversely, materials with M(III)/Cr(III) ratios <60/40 were highly porous solids. Binding energy measurements indicated that the insertion of mixed oxides into the phosphate matrix was topotactic and that strong interaction between the mixed oxide pillars and the phosphate surface occurred, particularly in the case of Al/Cr pillared compounds.

Calcination of the precursors was carried out under nitrogen, in order to avoid any formation of Cr_2O_3 on the external surface of the pillared materials, which is produced by a triple oxidation−segregation−reduction process of Cr(III). Only samples with high Fe(III)/Cr(III) ratios presented a shoulder in the XPS spectra at higher energy characteristic of the presence of Cr(VI).[58]

Mixed Al/Cr intercalation compounds were crystalline at room temperature, with high basal spacings between

25.7 and 42.1 Å. After calcination at 400 °C, free heights up to 25 Å were found. In contrast, Fe/Cr and Ga/Cr intercalates and pillared materials were generally amorphous, which suggests that mixed oligomeric species with different charges and sizes were simultaneously intercalated. Nevertheless, neither coprecipitation nor oxide segregation were detected, except for the case of Ga/Cr samples 80/20 and 90/10.

The mixed oxide pillared materials with M(III)/Cr(III) ratios <60/40 were, in general, mesoporous solids with a high contribution of micropores (of the order of 0.1 $cm^3\ g^{-1}$) and narrow pore size distributions. In particular, sample Al/Cr 40/60 was microporous (V_{microp} ~0.3 $cm^3\ g^{-1}$) with a unique pore diameter of 18 Å and a BET surface area of 500 $m^2\ g^{-1}$ (640 $m^2\ g^{-1}$ upon calcination in air). Conversely, materials with M(III)/Cr(III) ratios >60/40 presented BET surface areas lower than 200 $m^2\ g^{-1}$ and low micropore volumes (<0.1 $cm^3\ g^{-1}$); those containing the highest concentrations of either aluminum or gallium were rather nonporous solids.

Pillared Phosphates from Organometallic Pillar Precursors. *Silica-Pillared Metal(IV) Phosphates*. The pillaring methods described above have all made use of the hydrolysis of metal salts [$AlCl_3$, $GaCl_3$, $Cr(OAc)_3$, etc.] for the preparation of pillaring solutions containing polynuclear species where the metal atoms are linked via oxo or hydroxo bridges. Sol−gel methods using alkoxide precursors provide an alternative to this approach, not only by allowing closely controlled hydrolysis but also because depending on the degree of substitution on the alkoxide used, species of different dimensionality and carrying organic functions attached to the metal center are formed in solution. Thus chemically modified alkoxides $R_xSi(OR')_{4-x}$, after hydrolysis (to give $R_xSi(OH)_{4-x}$) and condensation (to give Si−O−Si siloxane bridges), form predominantly two dimensional networks for $x = 2$, and discrete three-dimensional entities for $x = 3$.[59] A variable parameter is introduced by the nature of R, which may be alkyl or aryl but must in all cases carry a basic function to facilitate intercalation in the layered phosphate. While the Si−C bond is resistant to hydrolysis under these mild conditions, more aggressive oxidative treatment will specifically break $Si-C_{sp^2}$ or $Si-C_{sp^3}$ bonds, which opens up the unexplored avenue of alternative methods to thermal procedures for inducing the pillaring reaction. It may also be seen that the use of bulky and/or multifunctional (more than one basic group) long-chain substituents will tend to increase the lateral spacing of the siloxane species within the interlayer region, a factor favorable for the production of interlayer porosity. Organometallic precursor species have been far less used than inorganic ions in intercalation chemistry in general and for the pillaring of layered phosphates in particular.

The intercalation of aminosiloxanes into α-ZrP was first described by Lewis,[60] although no surface area data were given, and the characterization of intercalated and silica cross-linked phosphates using ^{29}Si and ^{31}P MAS NMR by Klinowski,[61] who also reported their hexane adsorption properties. More recently, Clearfield[62] has obtained silica pillared ZrP of high surface area by using the propylamine-induced colloidal dispersion strategy described above for the synthesis of chromia pillared phosphates. In parallel, various new routes leading to porous α- and γ-structured silica pillared phosphates have been developed, including a chemical method of pillar-to-layer grafting.[63]

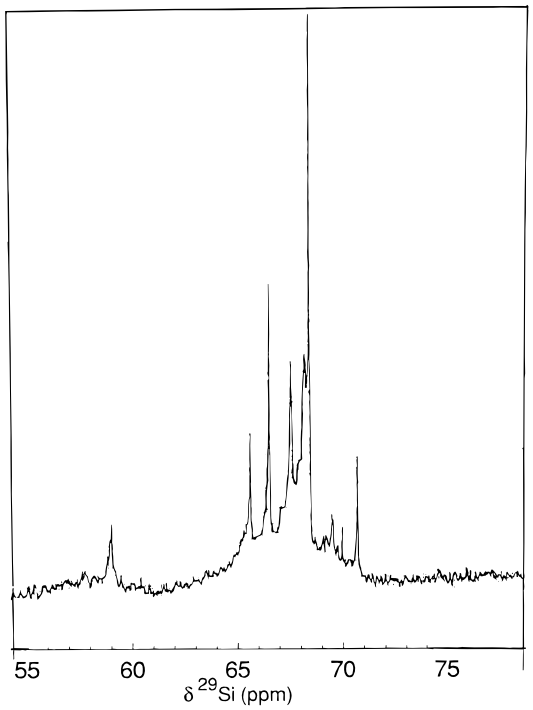

Figure 8. ^{29}Si NMR spectrum of ethanol/water solution (14/1) of (aminopropyl)triethoxysilane after 24 h aging (ppm from TMS).

Following the methods for the hydrolytic polycondensation of trifunctional monomers $XSiY_3$ to polyhedral oligosiloxanes described by Voronkov and Larent'yev,[59] the controlled hydrolysis of aminopropyltriethoxysilane in ethanol/water mixtures is seen to give the fully condensed octamer $[H_2N(CH_2)_3SiO_{1.5}]_8$ (**3**) as the predominant species, as identified by its ^{29}Si MAS NMR signal at −68.5 ppm from TMS,[64] Figure 8, and gel permeation chromatography.[65] The remaining signals in this spectrum arise from the presence of minor amounts of two incompletely condensed octamers **4** (−65.8, −66.7, and −68.4 ppm) and **5** (−59.1, −67.8, −69.7, −70.2, and −70.9 ppm), which decrease in intensity to the benefit of the resonance at −68.5 ppm with time. Facile intercalation occurs from such solu-

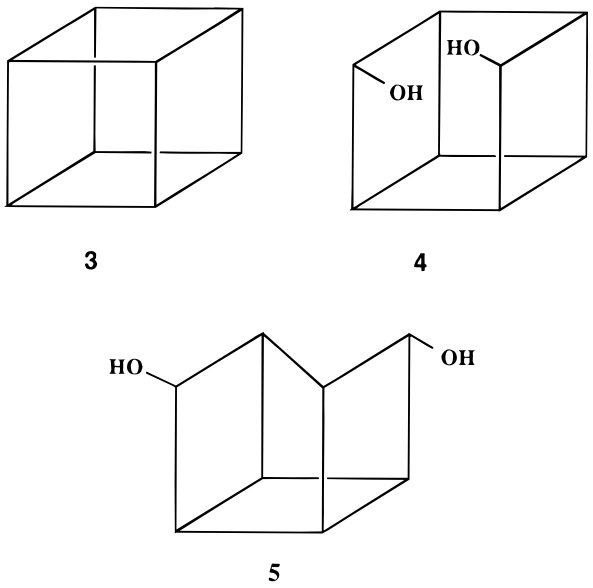

3 **4**

5

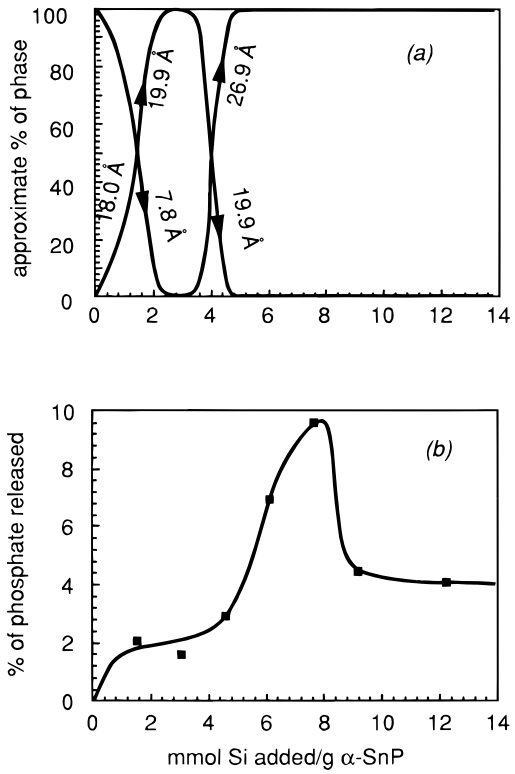

Figure 9. Intercalation of octakis(aminopropyl)siloxane into α-SnP. (a) Phase diagram: approximate percentage of each phase (from XRD). (b) Percent phosphate released as a function of the number of mmol of silicon present in solution/g of SnP.

tions into the layered phosphates. First studies using α-ZrP showed, however, that only low surface area materials could be obtained using a direct intercalation reaction. Detailed consideration[62,66] of the surface areas available per −POH site on the phosphate surface and that occupied by the siloxane octamer, in conjunction with the minimum uptake required to give a single-phase intercalation compound, showed that in fact the uptake was limited only by the covering effect and that a single layer of octameric units was inserted.[66] Together, this state of affairs produced a nonporous cross-linked structure after calcination. The challenge in this area was therefore identified as being 2-fold: to space out the siloxane pillar precursors laterally at the intercalation stage and/or to find synthetic conditions conducive to the formation of siloxane double layers. The success of one or other of these provides a means of modulating the pore size in directions parallel and perpendicular to the layers, which is one of the most important goals in tailored PLS chemistry.

Results obtained using $Sn(HPO_4)_2 \cdot H_2O$ provided a key to the answer.[66] Using α-SnP as host, the phase diagram plotted as a function of the amount of siloxane in solution (Figure 9a) shows that the system passes first through a monophasic region (interlayer distance 19.9 Å, siloxane monolayer), before destabilizing and rearranging to give a second phase of basal spacing 26.9 Å. As mentioned above, SnP is more susceptible to hydrolysis than ZrP and, indeed, phosphate is progressively released into solution as the system moves into the bilayer region, (Figure 9b). This release of phosphate, and the concomitant removal of active −POH sites by inactive Sn−OH groups, has the effect not only of increasing lateral spacing between pillars but also, more surprisingly, of allowing increased basal spacings by the formation of siloxane bilayers. Importantly, the

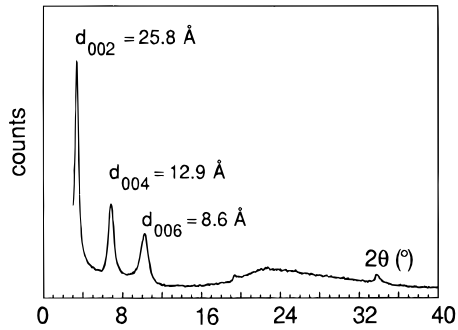

Figure 10. X-ray diffraction pattern of siloxane intercalated $Zr(HPO_4)_{1.4}(OH)_{1.2} \cdot nH_2O$.

increased free height is conserved after calcination and silica pillared SnP prepared in this way has a surface area of 230 $m^2\ g^{-1}$. The random removal of "active" −POH sites on SnP in basic solution has the effect of reducing the layer charge density, which is the stumbling block in the preparation of porous cross-linked phosphates. The high surface area silica pillared ZrP first reported by Clearfield was obtained using a propylamine dispersion of ZrP, which probably caused some elimination of phosphate groups.[62]

Reduction of the cation-exchange capacity can be performed in a more controlled fashion making use of methylamine, which shares with propylamine the particular property of acting as an exfoliating agent when in contact with aqueous suspensions of layered phosphates.[67] Its greater basicity, however, causes a further effect of hydrolysis of the exposed phosphate layers to a degree which is a function of the methylamine concentration, contact time and particle size of the metal(IV) phosphate. CEC-reduced ZrP, $Zr(HPO_4)_{2-x}(OH)_{2x} \cdot nH_2O$, the crystallinity of which is progressively lowered as x increases, is a novel host matrix for intercalation chemistry. Intercalation from octakis(aminopropyl)siloxane solutions leads to different phases from those obtained with pristine α-ZrP with expanded phases being obtained having basal spacings up to 28 Å (Figure 10), reminiscent of the results obtained using SnP. It can be concluded that a phosphate host of high layer charge density is capable only of including siloxane monolayers, whereas a lower layer charge density, combined with flocculation from a colloidally suspended host, allows double stacks to assemble.[63,68] This double layer is stable within a limited range of CEC-reduced ZrP, with less expanded phases being obtained above $x = 1$.

In addition, by varying the degree of CEC reduction, active −POH sites are increasingly further spaced, and a certain degree of control can be exercized over the pore size distribution, with the more hydrolyzed ZrP samples showing more mesoporous character. For example, whereas a silica pillared solid prepared from a modified ZrP with $x = 0.4$ has 80% of the BET surface area in micropores, the use of $Zr(HPO_4)(OH)_2 \cdot nH_2O$ leads to a solids in which 90% of the surface area results from mesopores. The highest surface area materials are those having the highest basal spacing after calcination, generally obtained with a CEC reduction of 20− 30%. Here, the surface area after calcination in air at 470 °C is 300−330 $m^2\ g^{-1}$ (Figure 11) and 190 $m^2\ g^{-1}$ at 550 °C, such a decrease in surface area as the temperature is increased being a generally observed phenomenon in PLS chemistry.

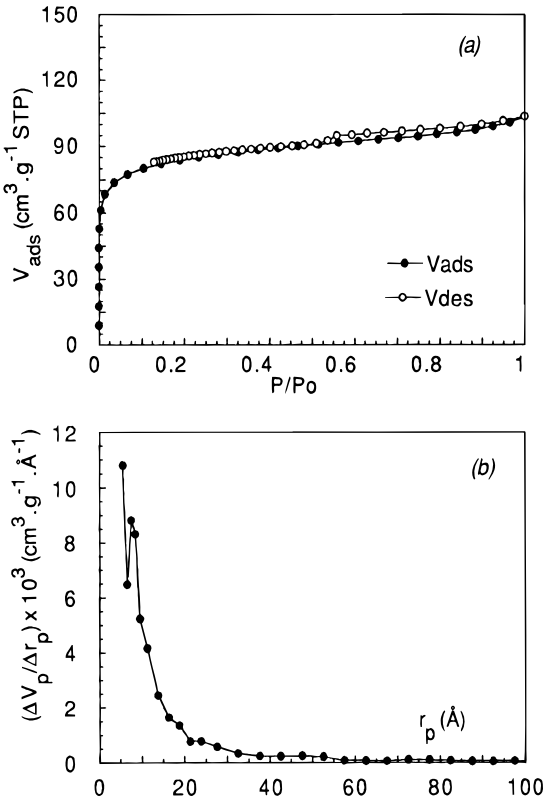

Figure 11. N_2 adsorption−desorption isotherm (a) and pore size distribution (r_p = pore radius) of silica-pillared $Zr(HPO_4)_{1.6}$-$(OH)_{0.8}\cdot nH_2O$. S_{BET} = 310 m^2 g^{-1}.

The use of bulkier substituents R in the alkoxide $RSi(OR')_3$ also has the potential of providing a means of pore size control, in particular when two or more amino functions per side chain allow anchoring to two or more phosphate groups. [*N*-(2-(aminoethyl)-3-aminopropyl)]-trimethoxysilane can be hydrolyzed in water−ethanol mixtures to give a sol in which the predominant species is the siloxane octamer (see above). The diamino functions promote interaction of each of the two cube faces parallel to the layers with eight active sites −POH, and not four, and the uptake of siloxane is limited accordingly, with a single-phased intercalation compound being observed by X-ray diffraction at half the silicon uptake required to give a single-phase material using octakis(aminopropyl)siloxane. The interlayer distance at this point indicates a monolayer, but using higher siloxane to ZrP ratios in solution a biphasic system with basal spacings of 18 and 24 Å is formed (Figure 12).[69] Possibly the hydrolysis of the phosphate layers at these increased amine:ZrP ratios is sufficient to enable the partial formation of a bilayer. This hypothesis would seem to be confirmed by other work in which the CEC of α-ZrP is reduced in a first stage by 10−15% using methylamine, after which a single-phase intercalation compounds of interlayer distance 20−24 Å are obtained. While this in itself represents another route to porous silica pillared materials, the particular advantage of the diaminosiloxane is the use of only some of its basic functions for intercalation purposes, the others being used to coordinate transition-metal ions. Cu^{II}, Co^{II}, Fe^{III}, and Ni^{II} were added as their nitrate salts to aged octakis(2-(aminoethyl)-3-aminopropyl)siloxane solutions and, on intercalation into $Zr(HPO_4)_{2-x}$-$(OH)_{2x}\cdot nH_2O$ (x = 0.2−0.4), the siloxane carries the transition metal ion into the interlayer region. After calcination at 440 °C, the materials are, in general, poorly crystalline, although ill-defined relections at low angle can still be distinguished. Interlayer spacings of heteroatomic Si−transition metal calcined phases are generally greater than those prepared under identical conditions but in the absence of metal ion: Si, 16.3; Si−Cu: 17.4; Si−Fe, 17.5; Si−Co, 21 Å.[70] Adsorption−desorption isotherms at 77 K are type I, with a hysteresis loop of type H4. Surface areas lie in the range 180−400 m^2 g^{-1}.

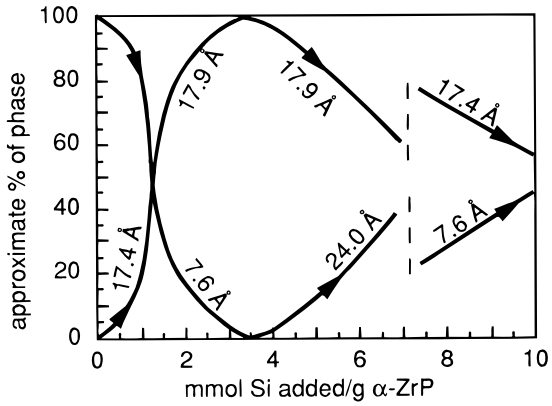

Figure 12. Approximate percentage of phases present on intercalation of octakis(2-(aminoethyl)-3-aminopropyl)siloxane into α-ZrP as a function of the number of mmol of Si present in solution/g of ZrP. The percentage of each phase present was determined by the relative intensity of the XRD lines.

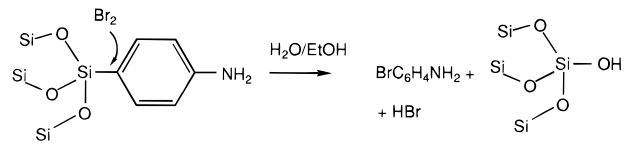

Figure 13. Schematic representation of oxidative rupture of $Si-C_{sp^2}$ bond by Br_2.

All of the examples given above make of α-structured ZrP. The γ-type structure differs quite significantly; the $Zr(PO_4)\cdot H_2PO_4$ layers are made up across their depth by $H_2PO_4-Zr-PO_4-Zr-H_2PO_4$,[71] and the two surface dihydrogen phosphate groups are of different acidity, causing a reduction in ion exchange capacity, generally half that of α-ZrP. In addition, the inorganic layer is thicker (9.3 Å) and has a greater rigidity. γ-ZrP has been used with much success for the preparation of γ-structured phosphonates by topotactic exchange with appropriate phosphonic acids. In the area of inorganic pillared compounds, Clearfield has reported an alumina pillared γ-TiP, prepared classically by ion exchange with Al_{13}^{7+}.[13]

The first silica pillared γ-ZrP was synthesized by intercalation from octakis(aminopropyl)siloxane solutions followed by calcination to remove the organic moiety and enable −POH−HOSi condensation.[64] The first stage in the development of "softer" chemical routes to PLS made use of intercalation from an (aminophenyl)siloxane sol, which enables chemically induced oxidative rupture of the $Si-C_{sp^2}$ bond, using bromine (Figure 13). ^{31}P MAS NMR indicates from the appearance of a resonance at −22 ppm from H_3PO_4 assigned to $P(OZr)_2$-$(OH)(OSi)$ groups that this low-temperature reaction is sufficient to initiate the grafting reaction, which is consolidated by heating to 450 °C, when the band at −22 ppm increases in intensity and another at −30 ppm and due to $P(OZr)_2(OSi)_2$ groups grows in progressively. Silica pillared γ-ZrP prepared in this fashion is particu-

larly thermally stable, retaining a surface area of 235 $m^2\ g^{-1}$ after thermal treatment at 650 °C, when a d_{002} diffraction line can still be identified, those samples calcined at 450−500 °C having higher BET surface areas of close to 300 $m^2\ g^{-1}$.

The phosphate layer charge can be reduced also by substituting a proportion of the P−OH groups by P−R (R = organic group),[72] as shown by Alberti et al.[14] The organic matter can be eliminated by calcination leaving empty space in the interlayer region. Layered α-Zr/Ti phosphate−phosphonates with variable layer charge have been used for preparing silica pillared structures from nonaqueous solutions of (aminopropyl)triethoxysilane. Pillared materials with BET surface areas up to 150 $m^2\ g^{-1}$ were obtained by this method.[73] To enhance the acidity of the silica pillars, mixed Al/Si oligomers have been intercalated into layered α-Zr/Ti phosphate−phosphonates from mixed hydrolyzed solutions of (aminopropyl)triethoxysilane and Al diisopropylacetylacetonate. XPS showed Al to be in a tetrahedral environment.[74]

Properties

Ion Exchange. As pillared materials possess open structures, a certain ion-exchange capacity, at least residual, would be expected. Studies[75a] on ion-exchange properties of pillared clays concluded that zirconia- and alumina-pillared bentonites show higher exchange capacities (both anionic and cationic) than the original clay, although such reactions can be accompanied by partial pillar dissolution when the pH is low (anion exchange) or high (cation exchange)[75b].

Cation-exchange capacities of alumina pillared phosphates for Co^{2+}, Ni^{2+}, and Cu^{2+} [32] confirm the accessibility of acid sites present in the porous structure, especially when samples are previously put in contact with ammonia, because the NH_4^+ formed is a better leaving group. The uptake order observed ($Ni^{2+} > Co^{2+} > Cu^{2+}$) suggests that the species exchanging into the alumina-pillared tin phosphate material are the hydrates, $M(H_2O)_6^{2+}$ ($M = Co^{2+}$, Ni^{2+}) and $Cu(H_2O)_4^{2+}$, and further infers ease of accessibility of ion-exchange sites after pillaring. Detailed spectroscopic study of the transition-metal ion-exchanged materials has also shown that the sites available differ according to the type of exchanger and that both are different from those present in the starting α-tin phosphate. Likewise chromia-pillared tin and zirconium phosphates[76] present cation exchange capacities of 0.5−2.0 mequiv g^{-1}, and silica pillared α-ZrP shows reversible ion exchange for Cu^{2+}, Zn^{2+}, and Cd^{2+}.[77] Uptake of cadmium may be important in the context of scavenging of toxic metals.

Polymerization of Organic Monomers. The cavities and interlayer pores and voids which characterize PLS can be considered as "microreaction chambers", the use of which is assisted by the acid sites which reside on the internal surfaces to position and orient incoming molecules. Whilst PLS are nanocomposite (layer + pillar components) materials, the solids which result from their use as a matrix for the confinement of small particles (metal clusters, metal sulfides, polymers) can be termed nano/nanocomposites.[78]

Both porous and layered materials[79−82] have previously been used as hosts for the intercalation and polymerization of N- and S-containing organic monomers as a means of synthesizing encapsulated polymer hybrid organic−inorganic materials. The uptake and polymerization of small molecules such as pyrrole provide a probe of pore accessibility, geometry, and acidity in pillared layered phosphates, in view of potential applications in several fields (including, but not confined to, catalysis).

Chemical analyses revealed the presence of high polypyrrole loadings into the cavities of porous pillared phosphates after only short times.[83] SEM micrographs were compatible with the confinement of polymer in the porous network. In copper-exchanged alumina pillared phosphates, optical spectra indicated the simultaneous presence of polypyrrole in neutral (transition at 1.2 eV) and bipolaron (0.75 eV) states. However, in chromia-pillared zirconium phosphate, two features observed at 1.97 and 2.69 eV are typical of bipolaron species. Conversely, XPS spectra indicate that two (and not more) types of species are formed, because all materials exhibit N 1s bands which can be attributed to a neutral and a charged nitrogen. The absence of conductivity, already observed in other hosts,[79] was attributed to the limited polymer chain length and the presence of an insulating matrix.

Encapsulation of Semiconductor Particles. Semiconductor aggregates of nanometer size are inherently unstable, tending to agglomerate in the absence of stabilizing agents. Pioneering work on the occlusion of semiconductors in zeolites[84] was followed by the growth of ZnSe, PbS, CdS, and CdSe particles 30−50 Å in diameter in zirconium bis(2-carboxyethylphosphonate).[18a] PLS provide a new family of porous solids for the size quantization of semiconductor particles, and studies have been made using alumina[85] and silica pillared[86] phosphates. When Zn^{2+}- and Cd^{2+}-exchanged silica pillared γ-ZrP and α-SnP were reacted with H_2S under strictly anhydrous conditions, ZnS and CdS were formed in situ. Bandgaps obtained from optical absorption spectra were significantly increased (ZnS, 4.3 eV; CdS, 3.1 eV) compared with those of the bulk (ZnS, 3.4; CdS, 2.4 eV) to values compatible with the presence of clusters of size 20−25 Å, which agrees with the average pore size distribution of the hosts used. EXAFS spectroscopy at the Zn and Cd edges showed both metal ions to be tetrahedrally coordinated in the exchanged precursor phases (before sulfidation). The change in the local environment after reaction with hydrogen sulfide was particularly clear for the former, where the Fourier transformed XAFS spectrum showed contributions to the first coordination shell from oxygen [r(Zn−O) = 1.93 Å) and sulfur [r(Zn−S) = 2.30 Å), nonbonded interactions with pillar silica and layer phosphorus and two Zn- - -Zn shells at 3.4 and 4.1 Å (Figure 14a). Using these structural data, a basic tetrahedral structural unit was suggested, in which sulfur atoms occupy central positions and which interconnect through windows in the pillar network to form more extended arrangements (Figure 14b).[86]

Electrical Conductivity of Alumina Pillared α-Tin Phosphate. Al_{13}-intercalated layered phosphates are protonic conductors, their conductivity surpassing 10^{-2} S cm^{-1} at 80 °C/100% relative humidity.[37] A systematic study[87,88] of the electrical properties of several alumina-pillared α-tin phosphates has been undertaken. These porous materials exhibit electrical behavior which can be fitted by supposing two contributions resulting from the existence of two kinds of pores,

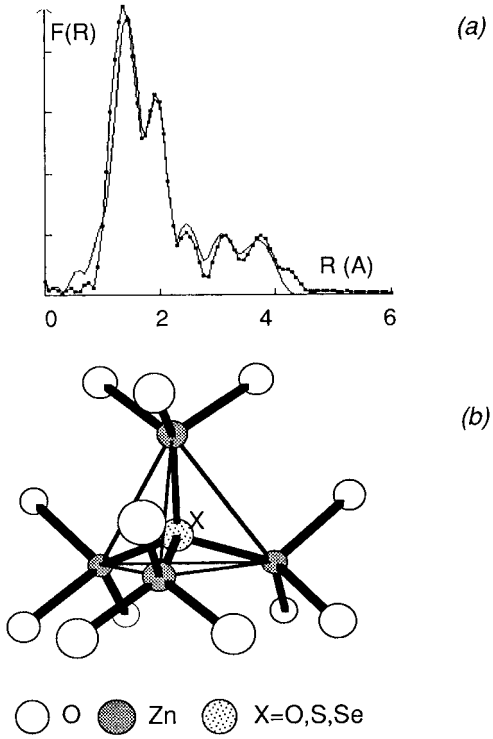

Figure 14. (a) Fourier transformed XAFS spectrum of $ZnS_{0.7}$ particles formed in situ in silica pillared γ-ZrP: (– · –) experimental and (—) calculated spectra. (b) Tetrahedral entity for occluded $ZnS_{0.7}$ compatible with the structural parameters derived from XAFS data.

interlayer micropores and small mesopores induced by pillaring, and mesopores resulting from edge–face interaction between layer packets. Lithium-exchanged alumina-pillared α-tin phosphate has a conductivity which decreases with temperature up to 260 °C and then increases gradually up to 500 °C. This behavior is interpreted by assuming the existence of two types of charge carrier: protons from zeolitic water, completely removed at 260 °C, and Li^+ ions. Theoretical models based on a coupling mechanism have been applied to explain the electrical behaviour of lithium-exchanged pillared phosphates.[89]

The electrical conductivity presents a marked dependence upon the lithium content. The activation energies, attempt frequency, and migration entropy[90] decrease with increasing basal distance, due to a lower interaction between diffusing ions themselves and with the pillars in larger pores.

Catalysis. Metal oxide pillared phosphates are solid acids with moderate or high Brønsted and Lewis acidity coming from acid sites located on both the phosphate surface and the pillar itself. Routine tests using thermal-programmed desorption of NH_3 and pyridine adsorption have shown that pillaring with metal oxides strongly enhances the acid properties of the layered phosphates in the range 100–600 °C, in which most catalytic reactions take place.

Isopropyl alcohol decomposition has been used as a probe of the acid properties of the catalytic sites in oxide pillared phosphates. Chromia pillared phosphates[91] possess active sites, acid and redox. Their relative thermal stability, specific surface area and the possibility of enlarging interlamellar distances between the phosphate layers by appropriate growth of chromia pillars enable them to be tailored as catalysts for specific reactions. In air, isopropyl alcohol is both dehydrated and dehydrogenated. As shown in Figure 15, the selectivity for one or other reaction could be modified by simply varying the chromium loading in the pillared phosphate.

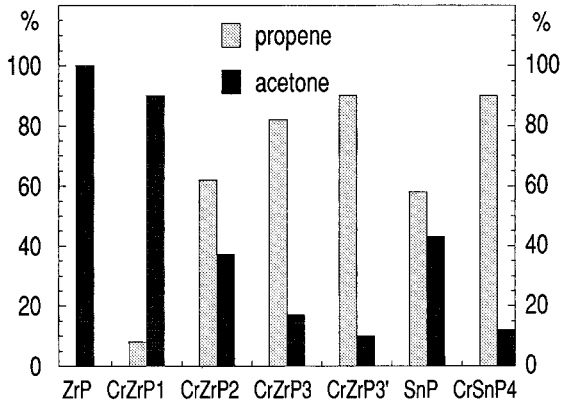

Figure 15. Selectivities to acetone and propene of α-SnP, α-ZrP, and chromia pillared materials calcined at 400 °C on decomposition of isopropyl alcohol at 180 °C in air. Chromia contents: **1**, 25.7%; **2**, 31.6%; **3**, 32.6%; **4**, 28.3%. CrZrP3′ calcined at 600 °C.

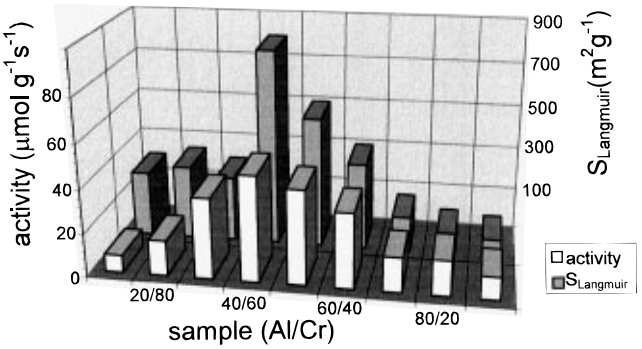

Figure 16. Comparison between activity for decomposition of isopropyl alcohol and surface area for Al/Cr pillared α-ZrP.

Fluorinated alumina pillared α-zirconium phosphate materials[38] displayed high catalytic activity for isopropyl alcohol decomposition, with a selectivity of practically 100% for the dehydration reaction. The presence of strong Lewis acid sites are believed to be mostly responsible for their catalytic properties.

Mixed alumina-chromia pillared α-zirconium phosphates[92] were found to be still more active catalysts, with catalytic activity up to 20 times that of their homologous chromia pillared compounds and 2–3 times that of fluorinated alumina pillared materials. All mixed oxide pillared compounds studied, independent of their composition, were exclusively dehydrating catalysts with selectivities toward propene higher than 99% (Figure 16). The decomposition of isopropyl alcohol is expected to occur predominantly inside large micropores and, as the most porous materials, those with intermediate Al/Cr ratios were the most active catalysts.

Although Al/Si pillared phosphate phosphonate materials were nonporous solids they displayed high activities—up to 40 μmol g^{-1} s^{-1}—for the dehydration of 2-propanol.[93]

Separation Processes. Dynamic sorption studies on an alumina pillared α-tin phosphate have shown it to be very efficient for separating hydrocarbons and derivatives at low temperatures, whereas at higher temperatures it shows enhanced acid-catalysis characteristics.[94]

Alumina pillared phosphates are also promising materials in the nuclear field since they are very efficient for separating tritiated and hydrogenated water, with surprisingly high distribution coefficients, and demonstrate a selective adsorption of tritiated water.[95] In particular, the distribution coefficients found for alumina pillared α-tin phosphates ranged between 1.7 and 3.95, which are higher than those of commercial zeolites.

Perspectives

In recent years, the position occupied by PLS in the area of porous solids has undergone considerable upheaval by the perspectives opened by MCM-type materials. When addressing the role of PLS in relation to mesoporous MCM41s consideration should be made of three of their principal characteristics: chemical composition and heteroatom inclusion, ion-exchange capacity, and pore size and distribution. Whereas in MCM41s the pore size can be quite strictly controlled by using templating routes, in oxide pillared phosphates and other hosts there is frequently a distribution of pore sizes spanning micropores−small mesopores; while for some applications this may be useful, better control of pore size distribution in PLS remains a synthetic challenge. MCM materials, and zeolites in general, are not nanocomposite solids, and this tends to restrict their ultimate chemical composition. For a nonsiliceous component to be included in an MCM framework, it must be introduced at the inital stage of the reaction, and only a small proportion of heteroatom can be fully incorporated into the silica matrix without its segregation as a distinct oxidic component. The insertion of metal oxide precursors by intercalation in a layered host matrix followed by the grafting reaction which characterizes the nanocomposite route to PLS creates framework chemical variety and in an atom concentration relative to the layer composition that cannot, yet, be achieved in other porous solids. The pore environment can be further modified by ion exchange since the retained ion exchange capacity of PLS is high. These considerations are clearly of importance in catalysis. PLS have a pivotal role to play in the spectrum of porous solids represented by microporous zeolites−PLS−MCM41 and other templated mesoporous materials, both by the variety of atom types that can be incorporated into the oxide pillar and the range of pore size dimension simultaneously present.

Acknowledgment. Financial support from the European Union Brite EuRam II program under the Concerted European Action on Pillared Layered Solids, Contract BRE2-CT93-0450, and personal bursary ERB-.BRE2-CT93-3005 (to P.M.T.) is gratefully acknowledged.

References

(1) Pinnavaia, T. J. *Science* **1983**, *220*, 365.
(2) Burch, R., Ed. *Catal. Today* **1988**, *2*, pp. 1−185.
(3) Figueras, F. *Catal. Rev. Sci. Eng.* **1988**, *30*, 457.
(4) Behrens, P. *Adv. Mater.* **1993**, *5*, 127.
(5) (a) *Multifunctional Mesoporous Inorganic Solids*; Sequeira, C. A. C., Hudson, M. J., Eds.; NATO ASI; Kluwer Academic: Dordrecht, 1993, 400. (b) *Pillared Layered Structures: Current Trends and Applications*; Mitchell, I. V., Ed.; Elsevier Applied Science: London, 1990.
(6) Hardin, S.; Hay, D.; Millikan, M.; Sanders, J. V.; Turney, T. W. *Chem. Mater.* **1991**, *3*, 977. (b) Hou, W.; Peng, B.; Yan, Q.; Fu, X.; Shi, G. *J. Chem. Soc., Chem. Commun.* **1993**, 253. (c) Anderson, M. W.; Klinowski, J. *Inorg. Chem.* **1990**, *29*, 3263.
(7) (a) Wong, S. T.; Cheng, S. *Chem. Mater.* **1993**, *5*, 770. (b) Dailey, J.; Pinnavaia, T. J. *Chem. Mater.* **1992**, *4*, 855.
(8) (a) Drezdzon, M. A. *Inorg. Chem.* **1988**, *27*, 4628. (b) Chibwe, K.; Jones, W. *Chem. Mater.* **1989**, *1*, 489. (c) Dimotakis, E. D.; Pinnavaia, T. J. *Inorg. Chem.* **1990,** *29*, 2393. (c) de Roy, A.; Forano, C.; El Malki, K.; Besse, J. P. In *Synthesis of Microporous Materials*; Occelli, M. L., Robson, H., Eds.; Van Nostrand Reinhold: New York, **1992**; pp 108−169. (d) Wang, J.; Tian, Y.; Wang, R. C.; Clearfield, A. *Chem. Mater.* **1992**, *4*, 1276.
(9) Beck, J. S.; Vartuli, J. C.; Roth, W. J.; Leonowicz, M. E.; Kresge, C. T.; Schmitt, K. D.; Chu, C. T.-W.; Olson, D. H.; Sheppard, E. W.; McCullen, S. B.; Higgins, J. B.; Schlenker, J. L. *J. Am. Chem. Soc.* **1992**, *114*, 10834.
(10) (a) Galarneau, A.; Barodawalla, A.; Pinnavaia, T. J. *Nature* **1995**, *374*, 529. (b) Luca, V.; MacLachlan, D. J.; Hook, J. M.; Withers, R. *Chem. Mater.* **1995**, *7*, 2220. (c) Cielsa, U.; Demuth, D.; Leon, R.; Petroff, P.; Stucky, G. D.; Unger, K.; Schüth, F. *J. Chem. Soc., Chem. Commun.* **1994**, 1387. (d) Reddy, K. M.; Moudrakovski, I.; Sayari, A. *J. Chem. Soc., Chem. Commun.* **1994**, 1059.
(11) (a) Gonzalez, F.; Pesquera, C.; Blanco, C.; Benito, I.; Mendioroz, S. *Inorg. Chem.* **1992**, *31*, 727. (b) Ohtsuka, K.; Hayashi, Y.; Suda, M. *Chem. Mater.* **1993**, *5*, 1823. (c) Petridis, D.; Bakas, T.; Simopoulos, A.; Gangas, N. H. J. *Inorg. Chem.* **1989**, *28*, 2439. (d) Yamanaka, S. *Ceram. Bull.* **1991**, *70*, 1056.
(12) Concerted European Action on Pillared Layered Solids, contract BRE.CT91.0462.
(13) Clearfield, A.; Roberts, B. D. *Inorg. Chem.* **1988**, *27*, 3237.
(14) (a) Alberti, G.; Costantino, U.; Vivani, R.; Zappelli, P. In *Mater. Res. Soc. Symp. Proc.* **1991**; *233*, 95−100. (b) Alberti, G.; Costantino, U.; Vivani, R.; Zappelli, P. In *Mater. Res. Soc. Symp. Proc.* **1991**, *233*, 101−106. (c) Alberti, G.; Costantino, U.; Allulli, S.; Tomassini, N. *J. Inorg. Nucl. Chem.* **1978**, *40*, 1113. (d) Alberti, G.; Costantino, U.; Mamottini, F.; Vivani, R.; Zappelli, P. *Angew. Chem., Int. Ed. Engl.* **1993**, *32*, 1357. (c) Alberti, G.; Murcia-Mascaros, S.; Vivani, R.; *Mater. Chem. Phys.* **1993**, *3−4*, 187. (d) Alberti, G.; Murcia-Mascaros, S.; Vivani, R. *Mater. Sci. Forum* **1994**, *152−153*, 87.
(15) Alberti, G. In *Multifunctional Mesoporous Inorganic Solids*; Sequeira, C. A. C., Hudson, M. J., Eds.; NATO ASI; Kluwer Academic: Dordrecht, 1993; Vol. 400, 179−190.
(16) Clearfield, A. In *Multifunctional Mesoporous Inorganic Solids*; Sequeira, C. A. C., Hudson, M. J., Eds.; NATO ASI; Kluwer Academic: Dordrecht, 1993; Vol. 400, 159−178.
(17) (a) Clearfield, A. In *Design of New Materials*; Clearfield, A., Cocke D. A., Eds.; Plenum Press: New York, 1986; pp 121−134. (b) Clearfield, A. *Comments Inorg. Chem.* **1990**, *10*, 89.
(18) (a) Cao, G.; Rabenberg, L. K.; Nunn, C. M.; Mallouk, T. E. *Chem. Mater.* **1991**, *3*, 149. (b) Dines, M. B.; DiGiacomo, P. M. *Inorg. Chem.* **1981**, *20*, 92. (c) Dines, M. B.; DiGiacomo, P. M.; Callahan, K. P.; Griffith, P. C.; Lane, R. H. Cooksey, R. E. In *Chemically Modified Surfaces in Catalysis and Electrocatalysis*; A.C.S. Symp. Ser.; Miller, J., Ed.; 1982; Vol. 192, pp 223−240.
(19) Clearfield, A.; Tindwa, R. M. *Inorg. Nucl. Chem. Lett.* **1979**, *15*, 251.
(20) Alberti, G.; Casciola, M.; Costantino, U. *J. Colloid Interface Sci.* **1985**, *107*, 256.
(21) Clearfield, A.; Smith, G. D. *Inorg. Chem.* **1969**, *8*, 431.
(22) Albertsson, J.; Oskarsson, A.; Tellgren, R.; Thomas, J. O. *J. Phys. Chem.* **1977**, *81*, 1574.
(23) (a) Alberti, G. In *Inorganic Ion-Exchange Materials*; Clearfield, A., Ed.; CRC Press: Boca Raton, FL, 1982. (b) Costantino, U. *Ibid*.; pp 111−132 and references therein. (c) Clearfield, A. *Chem. Rev.* **1988**, *88*, 125.
(24) Alberti, G.; Costantino, U. In *Inclusion Compounds*; Atwood, J. L., Davies, J. E. D.; MacNicol, D. D., Eds.; Oxford University Press: Oxford, 1991; Vol. 5, **1991**, pp 136−176.
(25) (a) Pillion, J. E.; Thompson, M. E. *Chem. Mater.* **1991**, *3*, 777. (b) Costantino, U.; Marmottini, F. *Mater. Chem. Phys.* **1993**, *35*, 193. (c) Ding, Y.; Jones, D. J.; Maireles-Torres, P.; Rozière, J. *Chem. Mater.* **1995**, *7*, 562.
(26) Monaci, A.; La Ginestra A.; Patrono, P. *J. Photochem. Photobiol. A* 1995, *83*, 63.
(27) Costantino, U.; Curini, M.; Marmottini, F.; Rosati, O.; Pisani, E. *Chem. Lett.* **1994**, *12*, 2215.
(28) Costa, M. C. C.; Johnstone, R. A. W.; Whittaker, D. *J. Mol.Catal. A−Chem.* **1995**, *103*, 155.
(29) Costantino, U.; Marmottini, F.; Curini, M.; Rosati, O. *Catal. Lett.* **1993**, *22*, 333.
(30) Johansson, G. *Acta Chem. Scand.* **1960**, *14*, 771.
(31) (a) Akitt, J. W.; Greenwood, N. N.; Khandeval, B. L.; Lester, G. R. *J. Chem. Soc., Dalton Trans.* **1972**, 609. (b) Bottero, J. Y.; Cases, J. M.; Flessinger, F.; Poirier, J. E. *J. Phys. Chem.* **1980**, *84*, 2933.
(32) Olivera-Pastor, P.; Jiménez-López, A.; Maireles-Torres, P.; Rodríguez-Castellón, E.; Tomlinson, A. A. G.; Alagna, L. *J. Chem. Soc., Chem. Commun.* **1989**, 751.
(33) Maireles-Torres, P.; Olivera-Pastor, P.; Rodríguez-Castellón, E.; Jiménez-López, A.; Tomlinson, A. A. G.; Alagna, L. *J. Mater. Chem.* **1991**, *1*, 319.

(34) Rodríguez-Castellón, E.; Olivera-Pastor, P.; Maireles-Torres, P.; Jiménez-López, A.; Sanz, J.; Fierro, J. L. G. *J. Phys. Chem.* **1995**, *99*, 1491.
(35) Fu, G.; Nazar, L. F.; Bain, A. D. *Chem. Mater.* **1991**, *3*, 602.
(36) Maireles-Torres, P.; Olivera-Pastor, P.; Rodríguez-Castellón, E.; Jiménez-López, A.; Tomlinson, A. A. G. European Patent RM 91A000603, 1991.
(37) Jones, D. J.; Leloup, J. M.; Ding. Y.; Rozière, J. *Solid State Ionics* **1993**, *61*, 117.
(38) Mérida-Robles, J.; Olivera-Pastor, P.; Jiménez-López, A.; Rodríguez-Castellón, E. *J. Phys. Chem.*, in press.
(39) Paparazzo, E.; Severini, E.; Jiménez-López, A.; Maireles-Torres, P.; Olivera-Pastor, P., Rodríguez-Castellón, E.; Tomlinson, A. A. G. *J. Mater. Chem.* **1992**, *2*, 1175.
(40) Wagner, C. D. *Practical Surfaces Analysis*; Briggs, E. D., Seak, M. P., Eds.; Wiley: New York, 1990; Vol. 1, pp 595−634.
(41) MacLachlan, S. J.; Bibby, D. M. *J. Chem. Soc., Dalton Trans.* **1989**, 895.
(42) Jiménez-López, A.; Maza-Rodríguez, J.; Olivera-Pastor, P.; Maireles-Torres, P.; Rodríguez-Castellón, E. *Clays Clay Miner.* **1993**, *41*, 328.
(43) Yan, Q. J.; Hou, W. H.; Chen, Y. S. *J. Chem. Soc., Chem. Commun.* **1995**, 1865.
(44) Maireles-Torres, P.; Olivera-Pastor, P.; Rodríguez-Castellón, E.; Jiménez-López, A.; Tomlinson, A. A. G. *J. Solid State Chem.* **1991**, *94*, 368.
(45) Maireles-Torres, P.; Olivera-Pastor, P.; Rodríguez-Castellón, E.; Jiménez-López, A.; Tomlinson, A. A. G. *J. Mater. Chem.* **1991**, *1*, 739.
(46) Giles, C. H.; McEwan, T. H.; Nakhwa, S. N.; Smith, D. *J. Chem. Soc.* **1960**, 3973.
(47) Cranston, R. W.; Inkley, F. A. *Adv. Catal.* **1957**, *9*, 143.
(48) Jones, D. J.; Rozière, J.; Maireles-Torres, P.; Jiménez-López, A.; Olivera-Pastor, P.; Rodríguez-Castellón, E.; Tomlinson, A. A. G. *Inorg. Chem.* **1995**, *34*, 4611.
(49) Bornholdt, K.; Corker, J. M.; Evans, J.; Rummey, J. M. *Inorg. Chem.* **1991**, *30*, 2.
(50) Manceau, A.; Charlet, L. *J. Colloid Interface Sci.* **1992**, *148*, 425.
(51) Bradley, S. E.; Kydd, R. A.; Colin, A. F. *Inorg. Chem.* **1992**, *31*, 1181.
(52) (a) Bergaya, F.; Barrault, J. In *Pillared Layered Structures: Current Trends and Applications*; Mitchell, I. V., Ed.; Elsevier Applied Science: London, 1990; p 167. (b) Komadel, P.; Doff, D. H.; Stucki, J. W. *J. Chem. Soc., Chem. Commun.* **1994**, 1243.
(53) Zhao, D.; Yang, Y.; Guo, X. *Inorg. Chem.* **1992**, *31*, 4727.
(54) Zhao, D.; Yang, Y.; Guo, X. *Zeolites* **1995**, *15*, 58.
(55) Olivera-Pastor, P.; Maza-Rodríguez, J.; Maireles-Torres, P.; Rodríguez-Castellón, E.; Jiménez-López, A. *J. Mater. Chem.* **1994**, *4*, 179.
(56) Pérez-Reina, F. J.; Olivera-Pastor, P.; Rodríguez-Castellón, E.; Jiménez-López, A.; Fierro, J. L. G. *J. Solid State Chem.* **1996**, *122*.
(57) Alcántara-Rodríguez, M.; Olivera-Pastor, P.; Rodríguez-Castellón, E.; Jiménez-López, A. *J. Mater. Chem.* **1996**, *6*.
(58) Moulder, J. F.; Stickle, W. F.; Sobol, P. E.; Bomben, K. D. *Handbook of X-Ray Photoelectron Spectroscopy*; Chastain, J., Ed.; Perkin-Elmer Corp.: Eden Prairie, MN, 1992.
(59) Voronkov, M. G.; Larent'yev, V. I. *Top. Curr. Chem.* **1982**, *102*, 199.
(60) Lewis, R. M.; Van Santen, R. A.; Ott, K. C. European Patent 159,756, 1989.
(61) Li, L.; Liu, X.; Ge, Y.; Li, L.; Klinowski, J. *J. Phys. Chem.* **1991**, *95*, 5910.
(62) Sylvester, P.; Cahill, R.; Clearfield, A. *Chem. Mater.* **1994**, *6*, 1890.
(63) Cassagneau, T.; Jones, D. J.; Maireles-Torres, P.; Rozière, J. In *Synthesis of Microporous Structures: Zeolites, Clays and Nanostructures*; Occelli, M. L., Kessler, H., Eds.; Marcel Dekker: New York, 1996; Chapter 31.
(64) Cassagneau, T.; Jones, D. J.; Rozière, J. *J. Phys. Chem.* **1993**, *97*, 8678.
(65) Schubert, U.; Hüsing, N.; Lorenz, A. *Chem. Mater.* **1995**, *7*, 2010.
(66) Rozière, J.; Jones, D. J.; Cassagneau, T. *J. Mater. Chem.* **1991**, *1*, 1081.
(67) Alberti, G.; Marmottini, F. *J. Colloid Interface Sci.* **1993**, *157*, 513.
(68) Jones, D. J.; Cassagneau, T.; Rozière, J., manuscript in preparation.
(69) Jones, D. J; Cassagneau, T.; Rozière, J. In *Multifunctional Mesoporous Inorganic Solids*; Sequeira, C. A. C., Hudson, M. J., Eds.; NATO ASI; Kluwer Academic: Dordrecht, 1993; Vol. 400, pp 289−302.
(70) Aptel, G.; Jones, D. J.; Rozière, J., unpublished results.
(71) (a) Christiansen, A. N.; Krogh Andersen, E.; Krogh Andersen, I. G.; Alberti, G.; Nielsen, M.; Lehmann, M. S. *Acta Chem. Scand.* **1990**, *44*, 865. (b) Poojary, D. M.; Shpeizer, B.; Clearfield, A. *J. Chem. Soc., Dalton Trans.* **1995**, 111.
(72) Farfán-Torres, E. M.; Maza-Rodríguez, J.; Martínez-Lara, M.; Jiménez-López, A. *Solid State Ionics* **1993**, *63−65*, 506.
(73) Martínez-Lara, M.; Farfán-Torres, E. M.; Santamará-González, A.; Jiménez-López, A. *Solid State Ionics* **1994**, *73*, 189.
(74) Santamará-González, J.; Jiménez-López, A.; Martínez-Lara, M. *J. Solid State Chem.* **1995**, *120*, 382.
(75) (a) Dyer, A.; Gallardo, T. *Recent Developments in Ion Exchange 2*; Williams, P. A., Hudson, M. J., Eds.; Elsevier: London, 1990; p 75. (b) Molinard, A.; Clearfield, A.; Zhu, H. Y.; Vansant, E. F. *Micropor. Mater.* **1994**, *3*, 109.
(76) Maireles-Torres, P.; Olivera-Pastor, P.; Rodríguez-Castellón, E.; Jiménez-López, A.; Tomlinson, A. A. G. *Recent Developments in Ion Exchange 2*; Williams, P. A., Hudson, M. J., Eds.; Elsevier: London, 1990; p 95.
(77) Skordilis, C.; Jones, D. J.; Rozière, J. *J. Mater. Chem.*, in press.
(78) Komarneni, S. *J. Mater. Chem.* **1992**, *2*, 1219.
(79) Bein, T.; Enzel, P. *Angew. Chem., Int. Ed. Engl.* **1989**, *28*, 1692.
(80) (a) Kanatzidis, M. G.; Tonge, L. M.; Marks, T. J.; Marcy, H. O.; Kannewurf, C. R. *J. Am. Chem. Soc.* **1987**, *109*, 3797. (b) Kanatzidis, M. G.; Marcy, H. O.; McCarthy, W. J.; Kannewurf, C. R.; Marks, T. J. *Solid State Ionics* **1989**, *32/33*, 594.
(81) Mehrotra, V.; Giannelis, E. P. *Solid State Ionics* **1992**, *51*, 115.
(82) Wu, C.-G.; Bein, T. *Chem. Mater.* **1994**, *6*, 1109.
(83) Maireles-Torres, P.; Olivera-Pastor, P.; Rodríguez-Castellón, E.; Jiménez-López, A.; Tomlinson, A. A. G. *J. Inclus. Phenom.* **1992**, *14*, 327.
(84) (a) Wang, Y.; Herron, N. *J. Phys. Chem.* **1987**, *91*, 257. (b) Herron, N.; Wang, Y.; Eddy, M. M.; Stucky, G. D.; Cox, D. E.; Moller, K.; Bein, T. *J. Am. Chem. Soc.* **1989**, *111*, 530. (c) Moller, K.; Bein, T.; Herron, N.; Mahler, W.; Wang, Y. *Inorg. Chem.* **1989**, *28*, 294.
(85) Jiménez-López, A.; Maireles-Torres, P.; Olivera-Pastor, P.; Rodríguez-Castellón, E.; Tomlinson, A. A. G. In *Multifunctional Mesoporous Inorganic Solids*; Sequeira, C. A. C., Hudson, M. J., Eds.; NATO ASI, Kluwer Academic: Dordrecht, **1993**; Vol. 400, pp 273−287.
(86) Cassagneau, T.; Hix, G. B.; Jones, D. J.; Maireles-Torres.; Rhomari, M.; Rozière, J. *J. Mater. Chem.* **1994**, *4*, 189.
(87) Criado, C.; Ramos-Barrado, J. R.; Maireles-Torres, P.; Olivera-Pastor, P.; Rodríguez-Castellón, E.; Jiménez-López, A. *Solid State Ionics* **1993**, *61*, 139.
(88) Criado, C.; Ramos-Barrado, J. R.; Maireles-Torres, P.; Olivera-Pastor, P.; Jiménez-López, A.; Rodríguez-Castellón, E. *Mater. Res. Soc. Symp. Proc.* **1993**, *286*, 347.
(89) Ramos-Barrado, J. R.; Criado, C.; Maireles-Torres, P.; Olivera-Pastor, P.; Rodríguez-Castellón, E.; Jiménez-López, A. *Solid State Ionics* **1994**, *73*, 67.
(90) Ramos-Barrado, J. R.; Criado, C.; Maireles-Torres, P.; Olivera-Pastor, P.; Rodríguez-Castellón, E.; Jiménez-López, A. *Mater. Res. Soc. Symp. Proc.* **1995**, *371*, 175.
(91) Guerrero-Ruiz, A.; Rodríguez-Ramos, I.; Fierro, J. L. G.; Jiménez-López, A.; Olivera-Pastor, P.; Maireles-Torres, P. *Appl. Catal. A* **1992**, *92*, 81.
(92) Olivera-Pastor, P.; Rodríguez-Castellón, E.; Maza-Rodríguez, J.; Jiménez-López, A. *J. Mol. Catal.*, in press.
(93) Santamará-González, J.; Martínez-Lara, M.; López-Granados, M., Fierro, J. L. G.; Jiménez-López, A. *Appl. Catal. A*, in press.
(94) (a) De Stefanis, A.; Perez, G.; Tomlinson, A. A. G. *J. Mater. Chem.* **1994**, *4*, 959. (b) De Stefanis, A.; Perez, G.; Ursini, O.; Tomlinson, A. A. G. *Appl. Catal. A* **1995**, *132*, 353.
(95) Maireles-Torres, P.; Olivera-Pastor, P.; Rodríguez-Castellón, E.; Jiménez-López, A.; Tomlinson, A. A. G.; Keyehan, Y.; Perez, G. European Patent RM 92A000376, 1992.

CM960156R